PSK Communications Systems using Fully Saturated Power Amplifiers

JIA LI, Member, IEEE

QINGCHONG LIU, Member, IEEE
Oakland University

Quasi-constant envelope phase-shift keying (PSK) is analyzed to assess its ability to overcome nonlinearities caused by fully saturated RF power amplifiers in communications systems. These modulations can achieve bit error rate (BER) performance comparable to linear BPSK in additive white Gaussian noise (AWGN) channel. Quasi-constant envelope offset quadrature PSK (OQPSK) is presented as a design example. At a BER = 10^{-5}**, the SNR degradation caused by fully saturated power amplifiers is 0.1 dB. The simulated BER matches analytically derived results. For a communications system employing the quasi-constant envelope OQPSK and a rate 1/2 convolutional code with** $K = 7$**, the demodulation performance is degraded by 0.25 dB at a** BER = 10^{-5} **when a fully saturated power amplifier is employed.**

Manuscript received February 23, 2004; revised July 18, 2005; released for publication November 2, 2005.

IEEE Log No. T-AES/42/2/876426.

Refereeing of this contribution was handled by T. F. Roome.

This work was supported in part by the National Science Foundation under Grants ANI-0112722 and CNS-0435341.

This paper was presented in part at the IEEE Military Communications Conference, Anaheim, CA, Oct. 7–10, 2002, and the 2003 Canadian Workshop on Information Theory, Waterloo, Ontario, May 18–21, 2003.

Authors' address: Dept. of Computer Science and Engineering, Oakland University, DHE 157, Rochester, MI 48309-4478, E-mail: (li4@oakland.edu).

I. INTRODUCTION

Recently, the practice in broadband wireless and satellite communications has challenged modulation theory. A broadband wireless or satellite network has to support a very large number of user terminals. To achieve such high system capacity and performance, broadband wireless and satellite networks require modulation methods that have high bandwidth efficiency and low bit error rates (BERs) at low implementation complexity. As data rates become much higher in broadband wireless and satellite networks, a user terminal has to transmit at higher power levels than in the existing wireless communication systems [1–3]. To reach the required high transmission power and high power efficiency, power amplifiers working in the fully saturated region must be employed [4–7]. However, they often cause severe nonlinear distortion to the signal. When the required bandwidth is hundreds of megahertz or larger, the best linear RF power amplifiers can also cause significant signal distortion [9].

Modulation methods that generate a constant envelope in the signal are preferred to be able to tolerate the power amplifier distortion [11]. Important early work in constant envelope modulation include minimum shift keying (MSK) described by Doelz and Heald in 1961 [12], and Gaussian minimum shift keying (GMSK) of Murota and Hirade in 1981 [13]. The power spectral density of GMSK can be much more compact than that of the MSK signal. However, the Gaussian shaped pulse in GMSK is not a Nyquist shape and brings intersymbol interference. The increased intersymbol interference causes demodulation performance degradation. For example, in the Groupe Speciale Mobile (GSM) system using GMSK of a standard time-bandwidth product WT_b = 0.3, the performance degradation is 0.46 dB below binary phase-shift keying (BPSK) performance [13]. More complicated sequence estimation is often needed in the demodulator to overcome the intersymbol interference [14]. This approach increases the receiver complexity and is not preferred by the latest broadband systems where the data rate can be hundreds of mega-bits per second [9]. In [14], it was shown that the SNR degradation is 0.24 dB below BPSK performance at BER = 10^{-5}, after employing a four-state Viterbi algorithm to handle the intersymbol interference in a GMSK system with $WT_b = 0.25$.

Predistortion methods have been widely studied to combat nonlinearity in RF power amplifiers [15–16]. These methods add inverse filters in front of the power amplifier so that the combination of the inverse filter and the power amplifier can produce less nonlinearity. In [9] it was shown that at BER = 10^{-5}, the SNR degradation caused by power amplifier distortion is 1 dB below BPSK, after counting the 1.4 dB gain achieved by predistortion in a broadband

satellite communication system employing quadrature phase-shift keying (QPSK) at 800 Mbit/s in 650 MHz Ka-band. The radio in [9] represents the best linearity achieved at such a wide bandwidth. As the SNR degradation is still 1 dB with the best predistortion, the question remains unanswered whether the BER performance for a communications system employing PSK and nonlinear power amplifiers can achieve near BPSK BER performance.

Recently the wireless and satellite communication industry has undertaken significant efforts to search for modulation methods with good performance and low implementation complexity [1–3]. In 1996 several new modulation methods based on PSK were described [1–3]. Herbst, et al. measured the power spectrum density and the uncoded BER of a standard offset QPSK (OQPSK) signal sent through a saturated radio in an additive white Gaussian noise (AWGN) channel [2]. The SNR was degraded by 2.5 dB compared with BPSK at a BER = 10^{-5}. Wildauer, et al. added a $\pi/2$ rad rotation to even-numbered chips of a code-division muliple access (CDMA) signal using QPSK [1]. At the output of a nonlinear power amplifier with 2 dB compression, the power spectral density was improved with respect to that of the QPSK in the CDMA standard IS-95. However, the spectral sidelobes are high and cause significant out-of-band emission.

In 1996 Liu proposed the quasi-constant envelope modulations OQPSK and $\pi/4$ QPSK [3]. These methods minimize the envelope fluctuation in the modulated signal through proper pulse shaping [3]. The constraint on the envelope of the modulated signal is relaxed from being strictly constant to being quasi-constant [3]. These methods can achieve high bandwidth efficiency and near BPSK demodulation performance at low complexity levels [3, 8]. The quasi-constant envelope OQPSK proposed in [3] was implemented in broaband terminals for satellite communication. It is also the modulation method implemented in an on-board switching IP-based broadband satellite communication network at 400 Mbit/s [17].

Combating power amplifier distortion is also critical for communication systems employing CDMA technology or orthogonal frequency division multiplexing (OFDM) [18, 19]. In [18], it is shown that parallel transmitted sequences and quasi-maximum likelihood detection can help overcome the distortion caused by a nonlinear amplifier in multicode wideband CDMA (WCDMA) systems. The effect of amplifier nonlinearity to OFDM systems employing QPSK and QAM is studied in [19]. The nonlinear amplifier models in [18] and [19] have very good linear ranges. The power amplifier model in this paper is for a fully saturated power amplifier and has no linear range. This is the case when the power amplifier is fully saturated for high dc-to-ac power conversion efficiency [4, 5].

This paper proposes a novel communication system using quasi-constant envelope PSK to overcome power amplifier distortion. Section II describes the system model. Section III describes the filtering requirements when a saturated power amplifier is employed in the transmitter. Section IV analyzes the impact of the power amplifier nonlinearity on the power spectral density. Section V presents a design example with simulated results. Section VI summarizes the results.

II. SYSTEM MODEL

The block diagram of a broadband wireless or satellite communication system employing a fully saturated power amplifier is shown in Fig. 1. The source data is converted from a serial stream to two parallel streams. The two parallel data streams are filtered by pulse shaping filters with an impulse response function $p(t)$. The quadrature channel data can be delayed by half a symbol time, i.e., $\tau_0 = 0.5T_s$, if OQPSK is employed. Otherwise, $\tau_0 = 0$. The output of the pulse shaping filter is fed into a radio. The baseband signal at the input of the radio is

$$s_b(t) = s_I(t) + js_Q(t) \tag{1}$$

where $s_I(t) = \sum_k d_{2k} p(t - kT_s)$ is the signal to be transmitted by the in-phase channel and $s_Q(t) = \sum_k d_{2k+1} p(t - kT_s - \tau_0)$ is the signal to be transmitted by the quadrature phase channel. Here $\{d_i \mid d_i \in \{-1, +1\}\}$ is the information sequence to be transmitted and T_s is the symbol time. The radio upconverts the baseband signal to a bandpass signal centered at the carrier frequency, which is the input signal to the power amplifier and can be written as

$$s_1(t) = s_I(t)\cos(2\pi f_c t + \phi_0) - s_Q(t)\sin(2\pi f_c t + \phi_0) \tag{2}$$

where f_c is the carrier frequency and ϕ_0 is the initial carrier phase. The power amplifier in the radio amplifies the signal to the desired transmission power. The output of the radio is transmitted through an AWGN channel.

We consider a communication system employing fully saturated power amplifiers. The fully saturated power amplifier deserves study for two main reasons. First, the instantaneous efficiency of practical power amplifiers usually achieves a maximum when it is operated with the gain compressed by about 3 dB [6]. Second, overcoming the nonlinearity caused by a fully saturated power amplifier helps to combat the nonlinearity introduced by power amplifiers operated with some linearity such as class-B and class-C. Fully saturated power amplifiers cause severe nonlinearity to nonconstant envelope signals [4–7]. If a system can utilize fully saturated power amplifiers, the system

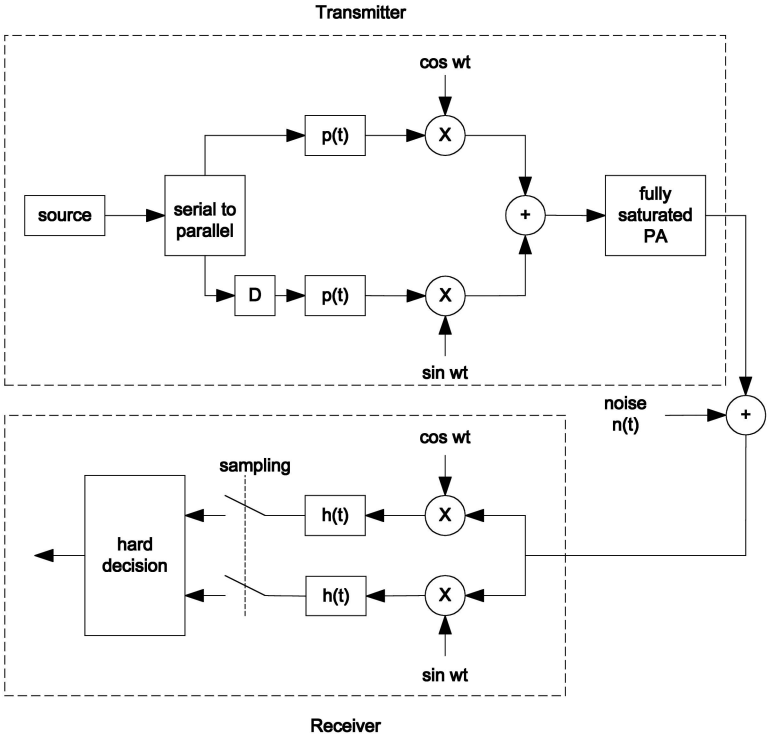

Fig. 1. Block diagram of communication system employing fully saturated RF power amplifier.

performance will become better when linear power amplifiers are employed.

A fully saturated power amplifier completely removes any amplitude information of its input signal. The phase of the output signal is approximately the same as the phase of the input signal. This has been verified by laboratory measurements and extensive simulations [3, 10]. One can assume that the fully saturated power amplifier does not change the phase trajectory of its input signal. Let $s_i(t)$ be the input signal to the power amplifier. The output signal $s_o(t)$ of the fully saturated power amplifier can be written as

$$s_o(t) = \begin{cases} 1 & \text{if} \quad s_i(t) > 0; \\ 0 & \text{if} \quad s_i(t) = 0; \\ -1 & \text{else.} \end{cases} \tag{3}$$

Therefore, it can be regarded as a ternary quantizer.

The fully saturated power amplifier is a nonlinear device which may generate harmonics of the carrier and distorts the transmitted signal envelope. In practical communication systems, the band-pass function of the phase lock loop in the power amplifier and upconverter module removes harmonics. Let the envelope of the input signal to the power amplifier be

$$\sqrt{s_I^2(t) + s_Q^2(t)} = 1 - y(t) \tag{4}$$

where $y(t)$ is the instantaneous deviation of the signal envelope. The function $y(t)$ is a random process determined by the information sequence and the shaping filter with impulse response $p(t)$ in Fig. 1.

The baseband equivalent signal for the transmitted signal can be written as

$$s_l(t) = s_b(t) + n_d(t) \tag{5}$$

where

$$n_d(t) = \frac{1 - \sqrt{s_I^2(t) + s_Q^2(t)}}{\sqrt{s_I^2(t) + s_Q^2(t)}} s_b(t) \tag{6}$$

represents the distortion caused by the fully saturated power amplifier. The distortion represents a random process which varys with the information sequence and shaping filter with impulse response $p(t)$. The distortion expands the power density spectrum [3, 21], makes it difficult to achieve high bandwidth efficiency, and causes degradation in demodulation performance.

Define the signal-to-distortion power ratio at the power amplifier output as

$$\gamma\{p(t)\} = E\left\{\frac{P_s}{P_d}\right\} \tag{7}$$

where

$$P_s = \lim_{T\to\infty} \frac{1}{2T} \int_{-T}^{T} |s_b(t)|^2 dt$$

$$P_d = \lim_{T\to\infty} \frac{1}{2T} \int_{-T}^{T} |n_d(t)|^2 dt$$

and the ensemble average is taken in the sample space for all possible information sequences. The signal-to-distortion power ratio $\gamma\{p(t)\}$ can serve as a fidelity metric for a saturated power amplifier.

Here the fully saturated power amplifier is treated as a ternary quantizer [22].

The signal-to-distortion power ratio represents the distortion to the desired signal at the power amplifier output. When a linear power amplifier is employed, $\gamma = \infty$. For constant envelope modulations such as MSK and GMSK, $\gamma = \infty$, when a fully saturated power amplifier is employed. In either case, $n_d(t) = 0$.

Assume the envelope of the input signal to a fully saturated power amplifier has a small variation, i.e., $\max|y(t)| \ll 1$. Substituting (4) into (6), the distortion can be written as

$$n_d(t) = s_b(t)\frac{y(t)}{1 - y(t)}. \tag{8}$$

Here $y(t)/(1 - y(t))$ is unitless. The signal-to-distortion power ratio can be increased by minimizing the power of $y(t)$ through choosing the appropriate shaping filter $\{p(t)\}$.

A modulation method using PSK is called a quasi-constant envelope PSK modulation method if it satisfies the following two conditions.

1) The envelope of the modulated signal at the output of a fully saturated power amplifier is not constant.

2) The modulated signal has $1 \ll \gamma < \infty$ at the output of a fully saturated power amplifier.

The receiver in the system model is a linear receiver as shown in Fig. 1. The received signal is down-converted to baseband, and the baseband signal is filtered by a filter with an impulse response function $h(t) = p(T_1 - t)$, where T_1 is the shaping pulse duration. This filter is matched to the shaping filter in the transmitter. The filter output is sampled and fed into a threshold detector.

In [21], it is recommended that the ideal demodulator should be a bank of filters for the different components of the nonlinear transmitter output. A bank of filters would add complexity to the receiver and increase the receiver cost.

III. OPTIMAL FILTERING

For the system in Fig. 1, it was widely believed that pulse shaping could not help much, because the fully saturated power amplifier completely removes the information contained in the envelope. It also seemed that it was impossible to achieve near-optimum linear BPSK bit error performance when the simplest linear demodulator was employed, because the fully saturated power amplifier causes too much distortion. A more complicated and powerful demodulator is needed to overcome the distortion [20, 21].

The following theorem shows that a special group of shaping pulses can help improve fully saturated power amplifiers and near-optimum linear BPSK bit error performance.

THEOREM 1 *In a communication system employing linear modulation with $p(t)$ as the pulse shaping function with a fully saturated power amplifier through an AWGN channel and linear demodulation filter matched to $p(t)$, the demodulation performance approaches the BPSK performance theory, i.e.,*

$$\lim_{\gamma\{p(t)\}\to\infty} P_b\{p(t)\} = Q\left(\sqrt{\frac{E_b}{\sigma^2}}\right) \tag{9}$$

where E_b/σ^2 is the signal-to-noise power ratio per bit, if and only if

1) $\gamma\{p(t)\} \to \infty$;

2) *the modulation filter $p(t)$ and the demodulation filter $h(t)$ satisfy the Nyquist pulse shaping criterion, i.e.,*

$$x(t = kT_s) = \begin{cases} 1 & k = 0 \\ 0 & k \neq 0 \end{cases}$$

where

$$x(t) = \int_{-\infty}^{\infty} p(\tau)h(t - \tau)d\tau. \tag{10}$$

In (9), the variance σ^2 is the variance of the AWGN only.

PROOF Let $a(t)$ be the impulse response function of the fully saturated power amplifier. The output of the power amplifier can be written as

$$s_a(t) = \int_{-\infty}^{\infty} s_b(\tau)a(t - \tau)d\tau. \tag{11}$$

When the first condition $\gamma\{p(t)\} \to \infty$ is true, we have

$$a(t) = a_0(t) + a_n(t) \tag{12}$$

where $a_0(t)$ is an ideal linear filter and $a_n(t)$ causes the power amplifier distortion. The receiver matched filter output is

$$r(t) = \int_{-\infty}^{\infty} (s_a(\tau) + n(\tau))h(t - \tau)d\tau. \tag{13}$$

For coherent PSK receivers, (13) can be rewritten as

$$r(t) = y(t) + n_1(t) \tag{14}$$

where

$$y(t) = \sum_k d_{2k}x(t - kT_s) + \sum_k d_{2k}g(t - kT_s) + j\left[\sum_k d_{2k+1}x(t - kT_s - \tau_0) + \sum_k d_{2k+1}g(t - kT_s - \tau_0)\right] \tag{15}$$

and

$$g(t) = \int_{\infty}^{-\infty} x(\tau)a_n(t - \tau)d\tau \tag{16}$$

and

$$n_1(t) = \int_{\infty}^{-\infty} n(\tau)h(t - \tau)d\tau \tag{17}$$

is the Gaussian noise with zero mean and variance $\sigma^2 = N_0/2$. When the second condition is true, the BER for coherent demodulation is bounded by

$$P_b\{p(t)\} \le Q\left(\sqrt{\frac{E_b}{\sigma_d^2+\sigma^2}}\right) \tag{18}$$

where σ_d^2 is the power of the distortion averaged in the in-phase channel and the quadrature channel. For a given signal-to-noise power ratio, i.e., E_b/σ^2 fixed, when the first condition is true, we have (9).

If the first condition is not true, then (12) does not hold. If the second condition is not true, the inequality (18) does not hold. Therefore, both conditions are necessary for (9) to hold.

The equality in (18) holds if the signal and distortion are independent. The dependence between the signal and the distortion becomes negligibly weak when the first condition in the theorem is true. In practical communications systems, the noise has a much higher power than the distortion at the matched filter output. For example, satellite communications systems usually require $E_b/N_0 \le 3$ dB, while the signal-to-distortion power ratio γ can be greater than 21 dB as shown in Section V.

The theorem holds for a communication system employing M-ary PSK with $M \le 4$. This includes BPSK, QPSK, and variations, such as OQPSK, $\pi/4$ QPSK, MSK, and GMSK. Analysis has shown that the theorem can be applied to 8 PSK. More study is needed for M-ary PSK when $M \ge 16$.

For communication systems employing PSK and a fully saturated power amplifier through an AWGN channel, the modulation method which achieves near optimal demodulation performance is a member of the quasi-constant envelope PSK modulation family.

The theorem says that when a fully saturated power amplifier is employed for an AWGN channel, near optimal demodulation performance can be achieved by employing the same filter as the pulse shaping filter and the receiver matched filter, which satisfy both the quasi-constant envelope modulated signal and the Nyquist filter constraints. Filtering is critical in both the transmitter and the receiver, when a nonlinearity is introduced by the transmitter. There are more functions $\{p(t)\}$, which satisfy either the first condition or the second condition in the theorem, respectively, but there are few functions that satisfy both conditions. Section V illustrates that functions satisfying both conditions exist.

IV. POWER SPECTRAL DENSITY

In this section, we show that the quasi-constant envelope PSK signal can help to reduce the distortion as seen in the power spectral density of the signal transmitted as the output of a fully saturated power amplifier.

For the system in Fig. 1, the autocorrelation function of the baseband equivalent transmitted signal is

$$\phi(t,t+\tau) = E\{s_l(t)s_l^*(t+\tau)\}. \tag{19}$$

Substituting (5) into (19), we have

$$\phi(t,t+\tau) = \phi_l(t,t+\tau) + \phi_d(t,t+\tau) \tag{20}$$

where

$$\phi_l(t,t+\tau) = E\{s_b(t)s_b^*(t+\tau)\} \tag{21}$$

is the autocorrelation function of the desired signal, and

$$\begin{aligned}\phi_d(t,t+\tau) = {} & E\{n_d(t)s_b^*(t+\tau) + s_b(t)n_d^*(t+\tau)\} \\ & + E\{n_d(t)n_d^*(t+\tau)\}\end{aligned} \tag{22}$$

is the correlation contributed by the distortion. Substituting (8) into (22), we have

$$\begin{aligned}\phi_d(t,t+\tau) = {} & E\left\{s_b(t)s_b^*(t+\tau)\frac{y(t)}{1-y(t)}\right\} \\ & + E\left\{s_b(t)s_b^*(t+\tau)\frac{y^*(t+\tau)}{1-y^*(t+\tau)}\right\} \\ & + E\left\{s_b(t)s_b^*(t+\tau)\frac{y(t)}{1-y(t)}\frac{y^*(t+\tau)}{1-y^*(t+\tau)}\right\}.\end{aligned}$$

This equation shows how the envelope variation $y(t)$ of the input signal affects the autocorrelation of the distortion $n_d(t)$ at the fully saturated power amplifier output. A challenging task is to find a useful analytical form for $y(t)$ since it can minimize the distortion power.

The function $\phi(t,t+\tau)$ is periodic in the t variable with period T_s. Assuming that the sequence of information symbols is wide-sense stationary, the baseband signal $s_l(t)$ is a periodic stationary process in the wide sense. Averaging $\phi(t,t+\tau)$ over a symbol period, we have

$$\bar{\phi}(\tau) = \frac{1}{T_s}\int_{-0.5T_s}^{0.5T_s}\phi(t,t+\tau)dt. \tag{23}$$

The power spectral density of the signal $s_l(t)$ is the Fourier transform of $\bar{\phi}(\tau)$, i.e.,

$$\Phi(f) = \int_{-\infty}^{\infty}\bar{\phi}(\tau)e^{-j2\pi f\tau}d\tau \tag{24}$$

which can be rewritten as

$$\Phi(f) = \Phi_l(f) + \Phi_d(f) \tag{25}$$

where

$$\Phi_l(f) = \frac{1}{T_s}\int_{-\infty}^{\infty}\int_{-0.5T_s}^{0.5T_s}\phi_l(t,t+\tau)e^{-j2\pi f\tau}dt\,d\tau \tag{26}$$

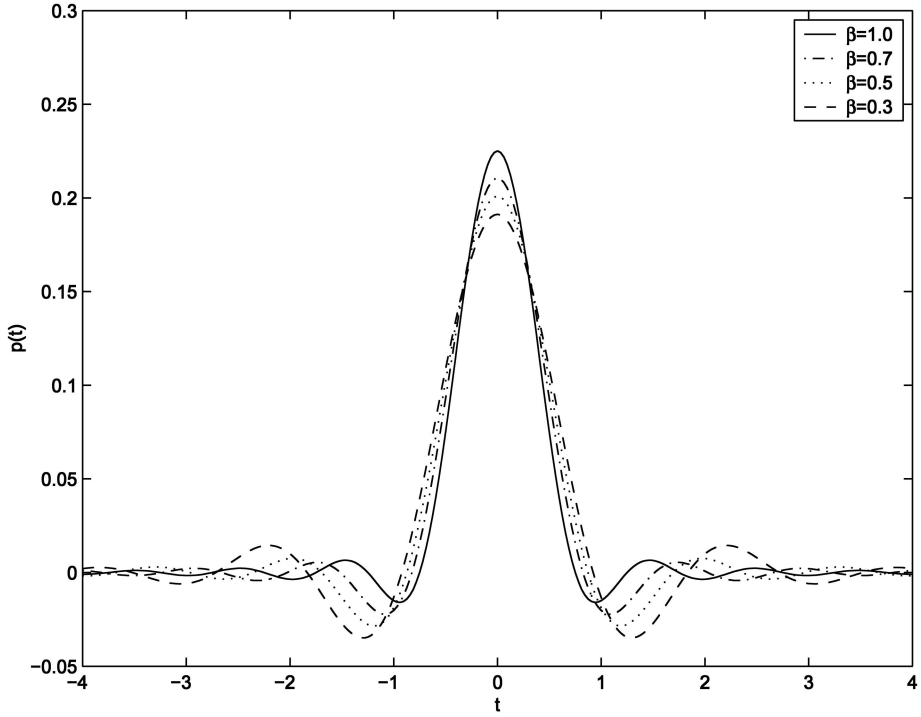

Fig. 2. Square root raised cosine function $p(t)$ with roll-off factor β.

TABLE I
Simulated Signal-to-Distortion Power Ratio γ of an OQPSK Signal Amplified by Fully Saturated Power Amplifier

	γ (dB)		
β	$L = 8$	$L = 6$	$L = 4$
1.0	21.38	21.33	21.34
0.9	19.86	19.81	19.84
0.8	18.43	18.37	18.40
0.7	17.11	17.06	17.06
0.6	15.92	15.89	15.85
0.5	14.84	14.83	14.80
0.4	13.88	13.87	13.90
0.3	13.03	13.05	13.17

Note: Square root raised cosine function with duration of L symbols and roll-off factor β.

is the power spectral density of the linear modulation, and

$$\Phi_d(f) = \frac{1}{T_s}\int_{-\infty}^{\infty}\int_{-0.5T_s}^{0.5T_s}\phi_d(t,t+\tau)e^{-j2\pi f\tau}dt\,d\tau \tag{27}$$

is the power spectral density contributed by the distortion.

When a linear power amplifier is employed, $n_d(t) = 0$, and $\Phi_d(f) = 0$. There is no distortion component in the power spectral density of the linearly modulated signal. When a nonlinear power amplifier is employed, $n_d(t) \neq 0$, $\Phi_d(f) \neq 0$ and contributes to the distortion component of the power spectral density.

The signal-to-distortion power ratio in (7) can be written as

$$\gamma = \frac{\int_{-\infty}^{\infty}\Phi_l(f)df}{\int_{-\infty}^{\infty}\Phi_d(f)df}. \tag{28}$$

In the AWGN channel, the transmission power is fixed for a given BER. In other words, the numerator in (28) is fixed. When quasi-constant envelope modulation is used, the signal-to-distortion power ratio is maximized. Therefore, the power in the distortion component is minimized.

V. DESIGN EXAMPLE: QUASI-CONSTANT ENVELOPE OQPSK

Quasi-constant envelope OQPSK is a subset of OQPSK modulations, which have $\gamma\{p(t)\} \gg 1$ and nonconstant envelope. Filter design, power spectral density, and simulated demodulation performance are presented for quasi-constant envelope OQPSK.

A. Filter Design

As shown in Section III, the filters which can produce the quasi-constant envelope signal and satisfy the Nyquist criterion are preferred. We consider the square root raised cosine function, which is a smooth function and traditionally employed to achieve high bandwidth efficiency with a linear RF power amplifier for the AWGN channel. This function also satisfies the Nyquist criterion. When it is used as both the impulse response function of the filters in the transmitter and the receiver, the matched filter

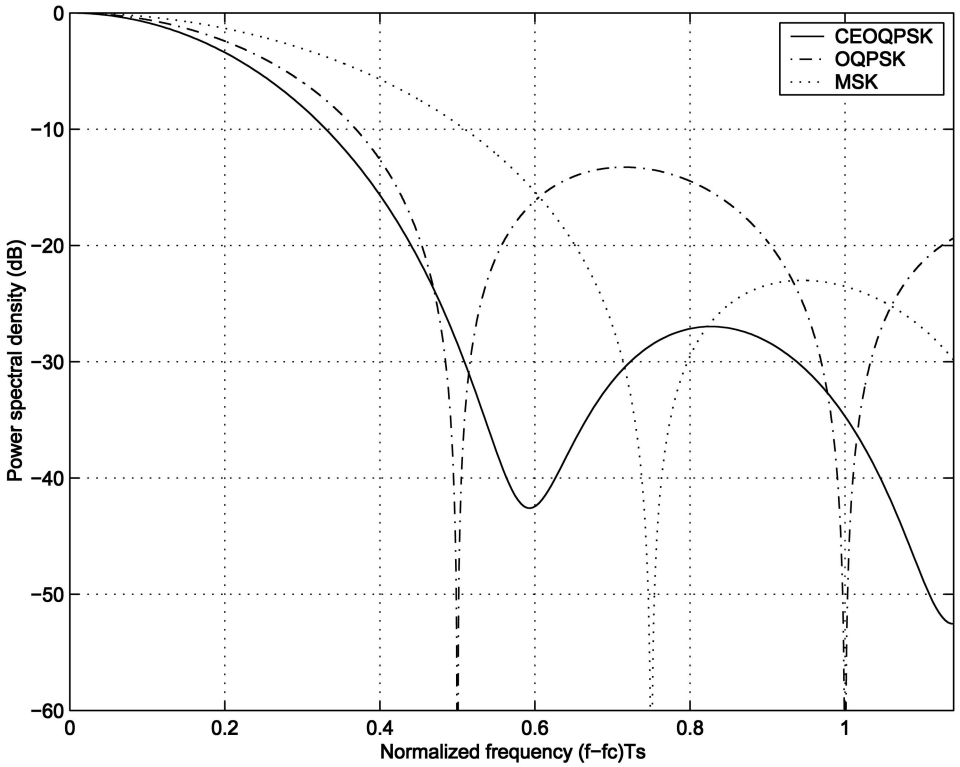

Fig. 3. Power spectral density of quasi-constant envelope OQPSK signal amplified by fully saturated power amplifier. Horizontal axis is normalized frequency $(f - f_c)T_s$, where T_s is symbol of time.

output is intersymbol-interference free, if a linear power amplifier is employed [23]. Ideal demodulation performance can be achieved in this case.

If the square root raised cosine function is employed as both the impulse response of the filter in the transmitter and the matched filter in the receiver for a fully saturated power amplifier, we need to ensure that the first condition of Theorem 1 can be satisfied, i.e., $\gamma \gg 1$.

Table I shows simulated results for the signal-to-distortion power ratio $\gamma\{p(t)\}$ for a system employing OQPSK. The signal-to-distortion power ratio $\gamma\{p(t)\}$ is derived using (5) and (7). The pulse shaping filter is of finite impulse response, which is a truncated version of the square root raised cosine function in Fig. 2. The duration of the filter is L symbols and the roll-off factor is β. It can be seen that the signal-to-distortion power ratio γ is highest when the roll-off factor is $\beta = 1.0$. The maximum value of the ratio γ is 21.38 dB. The effect of the shaping pulse duration L to the ratio γ is negligible.

B. Power Spectral Density

Fig. 3 shows a power spectral density analysis of the above quasi-constant envelope OQPSK signal amplified by a fully saturated RF power amplifier. The square root raised cosine function has a roll-off factor $\beta = 1.0$. The power spectral densities for OQPSK with a rectangular shaping pulse and for MSK are also plotted for comparison [23]. It can be seen that the power spectral density of the quasi-constant envelope OQPSK has a lower out-of-band power spectral density than either OQPSK or MSK. The OQPSK signal employing the rectangular shaping pulse has a constant envelope. Its pulse duration is one symbol. The random data causes abrupt phase changes and these result in high spectral sidelobes. The quasi-constant envelope OQPSK employs a smooth shaping pulse of a longer duration. The smoothness of the square root raised cosine function and its longer than one symbol-time duration help to smooth the baseband signal. Consequently the power spectral density has lower sidelobes. The smoothed baseband signal can thus tolerate the nonlinearity caused by the saturated power amplifier. The main spectral lobe of the quasi-constant envelope OQPSK signal is very close to the main spectral lobe of the OQPSK signal with rectangular shaping pulse. The quasi-constant envelope OQPSK compared with MSK gives similar results. At −43 dB, the mainlobe of the power spectral density for the quasi-constant envelope OQPSK is only 77% of the width of the mainlobe of the MSK power spectral density. Employing the quasi-constant envelope OQPSK saves 23% of the bandwidth compared to MSK.

In [9] the measured power spectral density was reported for broadband satellite communication systems, and these results were superior to results in [1] and [2]. The system in [9] employed QPSK at

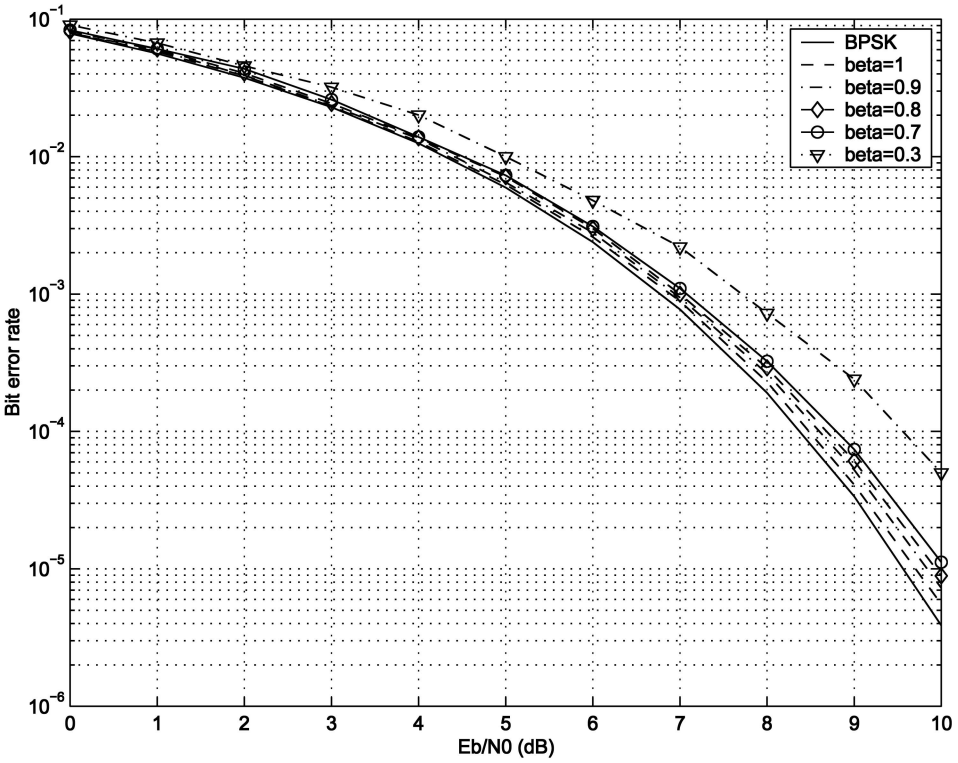

Fig. 4. Simulated BER of quasi-constant envelope OQPSK. Shaping filter impulse response in transmitter is square root raised cosine function with duration of 8 symbols.

800 Mbit/s in the 650 MHz Ka-band channel with a linear power amplifier working at −7 dB below saturation. The floor of the power spectral density was −20 dB below the peak of the mainlobe. The first sidelobe occurred at about −15 dB. When the quasi-constant envelope OQPSK is employed in a comparable system, it can achieve a saving of 38.25% of the system bandwidth, or equivalently 250 MHz. This saving of bandwidth can be achieved by employing quasi-constant envelope OQPSK at 400 Mbit/s in 400 MHz bandwidth.

C. Demodulation Performance

The optimal receiving filter for a nonlinear channel requires a bank of matched filters each followed by an infinite-length transversal filter [20]. To minimize receiver complexity, we consider using the same linear receiver for OQPSK used in linear channels, and investigate the demodulation performance of the quasi-constant envelope OQPSK transmitted by a fully saturated power amplifier in the AWGN channel.

As shown in Fig. 1, the chosen receiver is a linear receiver. The in-phase signal $\Re\{r(t)\}$ is filtered by the matched filter with the impulse response $p(T_1 - t)$, which is a square root raised cosine filter and is the same as the pulse shaping filter impulse response in the modulator. The quadrature phase signal $\Im\{r(t)\}$ is filtered by a matched filter with the same impulse response function $p(T_1 - t)$. Both matched filters are finite impulse response. The output of the matched filter is given in (14). The Gaussian noise in (14) has zero-mean and variance $\sigma^2 = N_0/2$. The output of the in-phase channel matched filter is sampled at time instants $2kT_b$, where T_b is the bit time. The output of the quadrature channel matched filter is sampled at time instants $(2k + 1)T_b$. A hard decision is made on both the in-phase channel and the quadrature channel samples.

Figs. 4, 5, and 6 show the simulated BER for coherent demodulation. The durations of both the pulse shaping filter and the matched filter are $L = 8$, 6, or 4 symbols. The BER for BPSK in a traditional AWGN channel is shown as a reference. In Fig. 4, it can be seen that at a BER of 10^{-5}, the SNR degradation is approximately 0.1 dB, when the duration of the filter is 8 symbols and the roll-off factor is $\beta = 1$. The degradation increases as the roll-off factor β decreases. For $\beta = 0.3$, the SNR degradation is approximately 1.2 dB at a BER of $5 \cdot 10^{-5}$.

In Fig. 5, it can be seen that the SNR degradation at a BER of 10^{-5} is approximately 0.15 dB, when the duration of the filters is 6 symbols and the roll-off factor is $\beta = 1$. For $\beta = 0.3$, the SNR degradation is 1.3 dB at a BER of 10^{-4}.

In Fig. 6, it can be seen that the SNR degradation at a BER of 10^{-5} is also 0.15 dB, when the duration of the filters is 4 symbols and the roll-off factor is $\beta = 1$. For $\beta = 0.3$, the SNR degradation is approximately 1.6 dB at a BER of 10^{-4}.

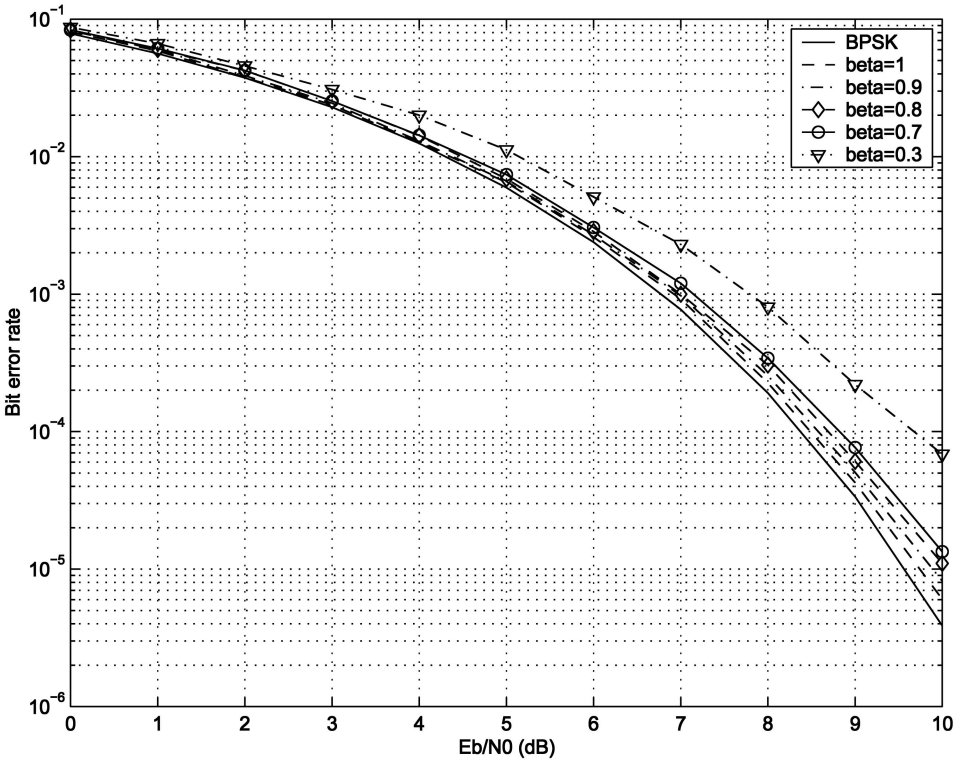

Fig. 5. Simulated BER of quasi-constant envelope OQPSK. Shaping filter impulse response in transmitter is square root raised cosine function with duration of 6 symbols.

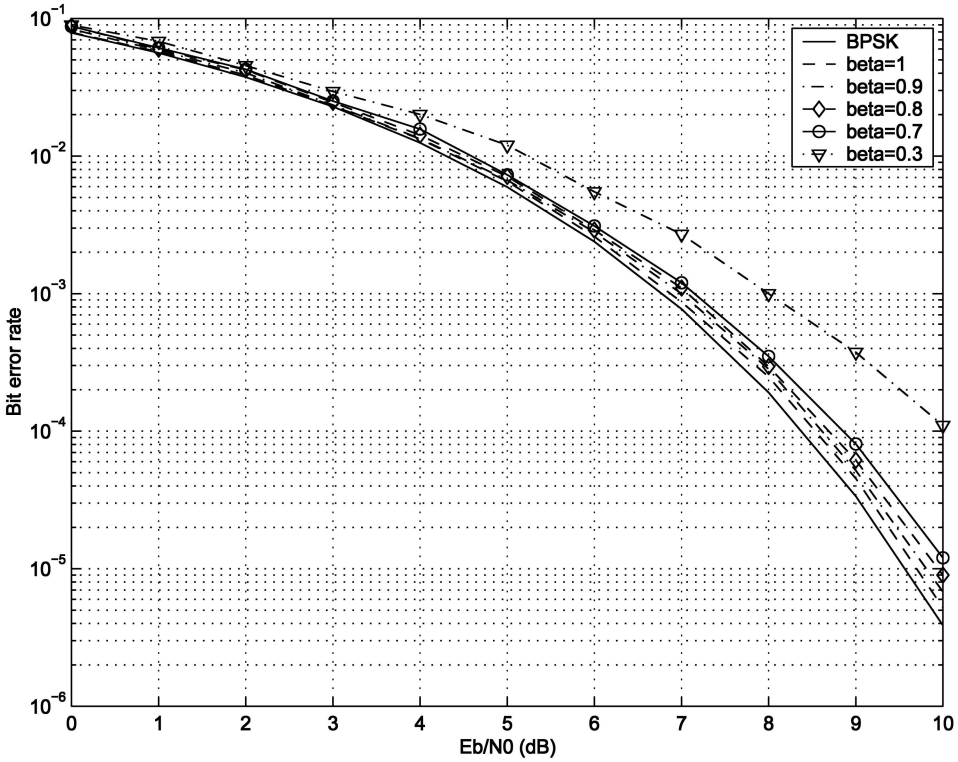

Fig. 6. Simulated BER of quasi-constant envelope OQPSK. Shaping filter impulse response in transmitter is square root raised cosine function with duration of 4 symbols.

When a linear receiver and a hard decision are employed, the quasi-constant envelope OQPSK can achieve demodulation performance close to BPSK. For $0.7 \leq \beta \leq 1$, increasing the shaping pulse duration to more than 4 symbols does not bring improvement in the BER performance. This is because

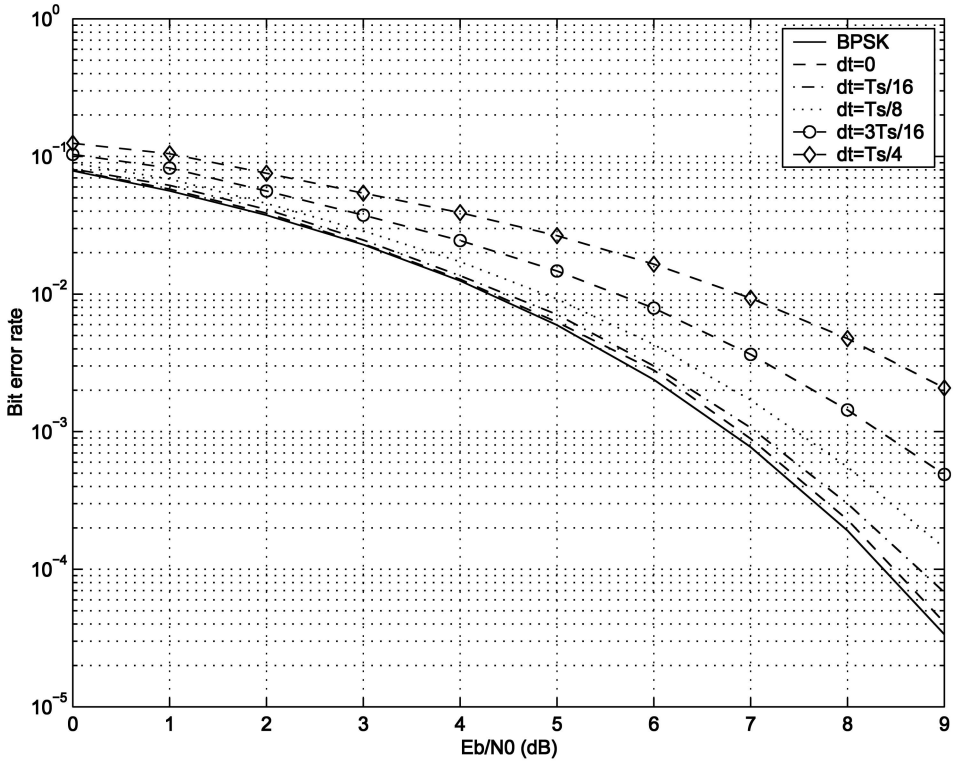

Fig. 7. Simulated BER of quasi-constant envelope OQPSK for different timing errors. Timing error is fixed for each curve. Shaping filter impulse response in transmitter is square root raised cosine function with $\beta = 1.0$ and duration of 6 symbols.

the fluctuation in the modulated signal envelope is small and the higher duration shaping pulse produces a negligible difference in smoothing the signal. For $\beta = 0.3$, increasing the duration can improve BER performance. When β is small, the fluctuation in the signal envelope is large and the higher duration pulse can smooth the signal. In practice, we recommend β between 0.7 and 1.0, and a shaping pulse duration of 6 symbols.

Our simulations have shown that the BER is an even function of the timing error, similar to a linear channel. Fig. 7 shows the simulated BER versus SNR for different timing errors. It can be seen that the timing error dt can cause a large degradation in SNR, when $|dt| > T_s/16$. Therefore, a symbol timing estimator with the standard deviation not larger than $T_s/16$ is needed.

In [25], it was shown that the Cramer-Rao bound for maximum likelihood symbol timing estimation is

$$\left(\frac{\sigma_\tau}{T_b}\right)^2 = \frac{1}{2T_\tau(P/N_0)(T_bD)^2} \tag{29}$$

where $T_\tau = NT_s$, and N is the number of symbols used for the timing estimation, P is the average power, $N_0/2$ is the power of the AWGN and

$$(T_bD)^2 = \frac{\pi^2}{12} + \left(\frac{\pi^2}{4} - 2\right)\beta^2. \tag{30}$$

Therefore, the number of symbols needed for symbol estimation such that $\sigma_\tau \le T_s/16$ is

$$N \ge \frac{16}{\frac{E_b}{N_0}\left[\frac{\pi^2}{12} + \left(\frac{\pi^2}{4} - 2\right)\beta^2\right]}. \tag{31}$$

Phase error can be caused by either the phase estimator or the phase-locked loop used for carrier recovery in the demodulator. When phase error is present, the matched filter output can be written as

$$r(t) = y(t)e^{j\theta} + n_1(t) \tag{32}$$

where $y(t)$ is given in (15), θ is the phase error, and $n_1(t)$ is the complex AWGN component with zero mean and variance $\sigma^2 = N_0/2$. Hard decision detection is applied to the matched filter output signals in the in-phase channel and quadrature channel.

Equation (32) can be rewritten as

$$\begin{aligned} r(t) = {} & y_I(t)\cos\theta - y_Q(t)\sin\theta \\ & + j[y_Q(t)\cos\theta + y_I(t)\sin\theta] + n_1(t) \end{aligned} \tag{33}$$

where $y_I(t) = \Re\{y(t)\}$ is the real part of $y(t)$ and $y_Q(t) = \Im\{y(t)\}$ is the imaginary part. Following the approach in Section III, the BER of quasi-constant envelope OQPSK in the presence of phase error is

$$P_b = Q\left(\sqrt{\frac{E_b\cos^2\theta}{\sigma^2 + \sigma_d^2 + E_b\sin^2\theta}}\right) \tag{34}$$

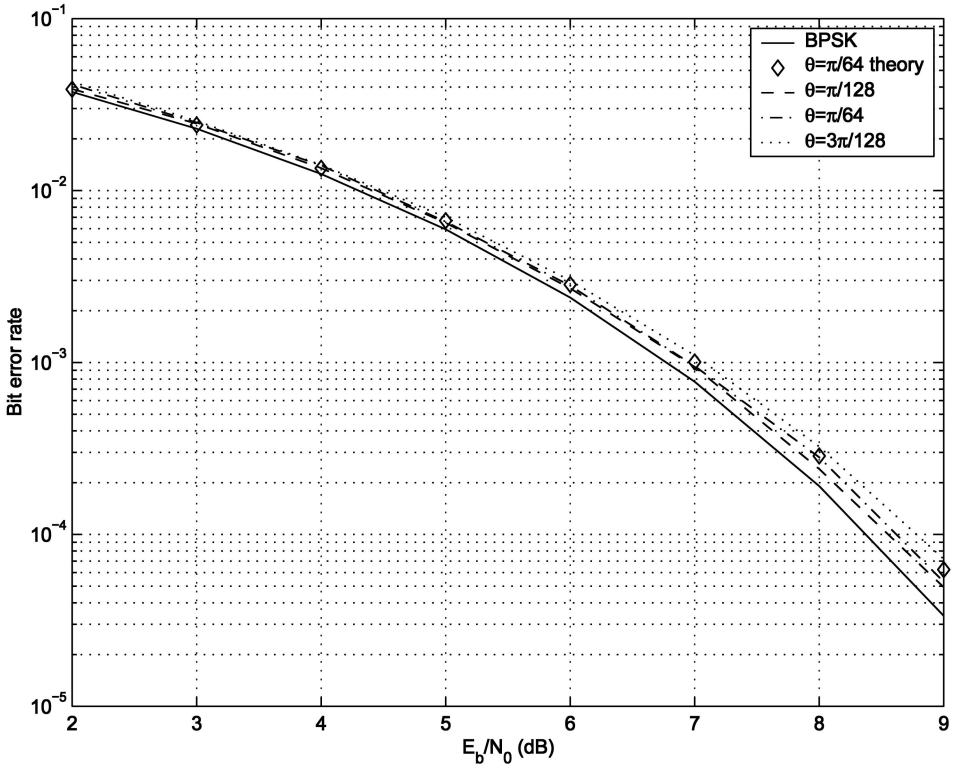

Fig. 8. Simulated BER for different phase errors. Solid line is BPSK modulation for comparison. Diamond points are calculated according to (34).

where σ_d^2 is the power of the distortion introduced by the fully saturated power amplifier.

Fig. 8 plots the simulated BER versus SNR for different phase errors. The BER is sensitive to phase errors. When the phase error is $\pi/64$, the SNR degradation is 0.2 dB at a BER of 10^{-4}. A phase estimator is often employed in the receiver for initial phase estimation. We recommend that the standard deviation of the phase estimator be less than $\pi/64$. It can also be seen that the simulated BER matches the result in (34).

In [25], it is shown that the Cramer-Rao bound for the unbiased maximum likelihood phase estimator is

$$\sigma_\phi^2 \geq (4NE_b/N_0)^{-1} \tag{35}$$

where N is the number of symbols employed for phase estimation.

In broadband wireless communications, a preamble is usually employed for packet detection and parameter estimation. It is common to see system specifications which require the SNR degradation by either the phase error or the timing error be not greater than 0.2 dB. The length of the symbols required for phase and timing estimation can be chosen according to (31) and (35). The simulated results shown in Fig. 8 are needed for the phase-locked loop design in a carrier recovery scheme and can be designed properly by following [26] and [27].

D. Coded Performance

The performance degradation caused by a fully saturated power amplifier for a coded system needs to be studied. The effect of channel distortion on BER is worse for a coded versus an uncoded communication system [27]. The BER of coded system decreases much faster than uncoded systems as SNR increases. Since the fully saturated RF power amplifier causes distortion (intersymbol interference), we expect the SNR degradation of the coded performance of the quasi-constant envelope OQPSK to be higher than that of the uncoded signal.

Convolutional coding is a reliable error correcting method for satellite and wireless communications. Broadband wireless and satellite communication systems are designed to provide services including high speed data communications. They require coding methods to achieve very low BER. Since the data rate is very high, complicated decoding methods are unaffordable in most applications. Convolutional codes of short constraint length are preferred in these systems.

The rate 1/2 convolutional code with the constraint length $K = 6$ or 7 was evaluated for communication systems employing the quasi-constant envelope OQPSK and fully saturated RF power amplifiers. The demodulator employs linear filters matched only to linear pulse shaping filters. The decoder is a Viterbi decoder using full precision soft decision

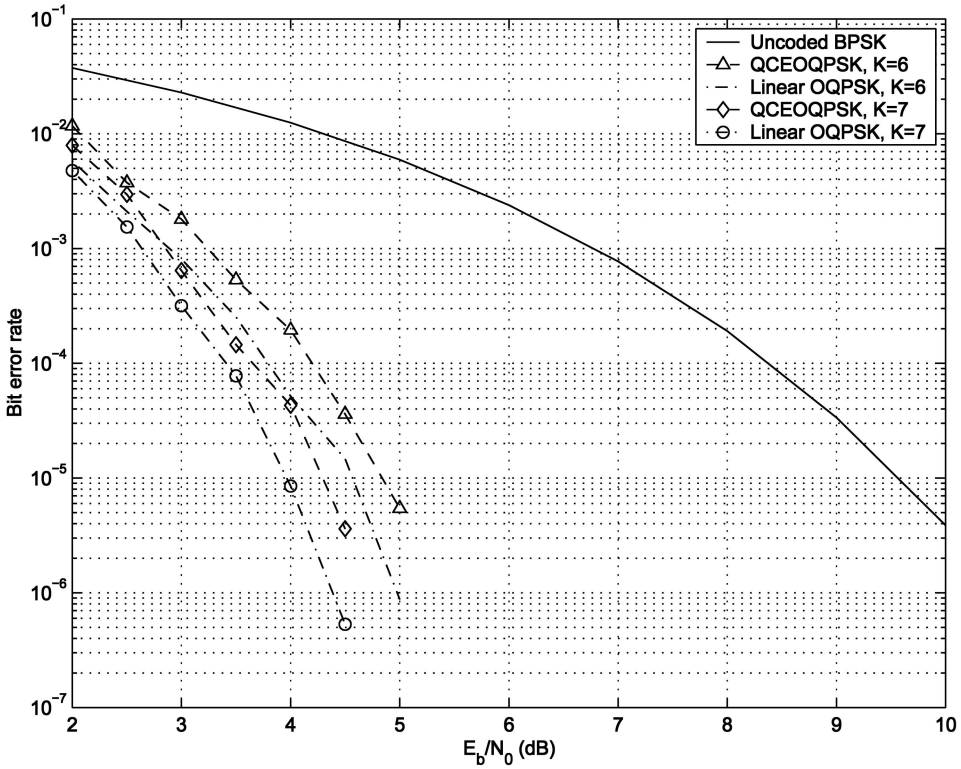

Fig. 9. Simulated BER of communication systems employing quasi-constant OQPSK through fully saturated power amplifiers and AWGN channel. Rate 1/2 convolutional code is employed with Viterbi decoder and full precision soft decoding. Solid line is ideal BER for BPSK. Code constraint lengths of $K = 6$ and $K = 7$ are shown. BER for linear power amplifiers with $K = 6$ and $K = 7$ are shown for comparison.

decoding. Fig. 9 shows the simulated BER result in an AWGN channel. The simulated BER for a system employing the ideal linear RF power amplifier is also shown for comparison. The simulated BER for the system employing the ideal linear RF power amplifier in an AWGN channel matches the coded performance for BPSK in [27]. It can be seen that the fully saturated RF power amplifier causes some small SNR degradation. When the BER is 10^{-5}, the degradation is about 0.25 dB. This is slightly larger than the SNR degradation for $\beta = 1.0$ in Fig. 4 for an uncoded system. Increasing the constraint length from $K = 6$ to $K = 7$ does not reduce the degradation. The SNR degradation caused by the fully saturated RF power amplifier is tolerable in practical broadband wireless and satellite communications systems.

VI. CONCLUSIONS

Quasi-constant envelope PSK is proposed and evaluated to achieve near optimal performance in broadband wireless and satellite communications systems employing fully saturated power amplifiers. Quasi-constant envelope PSK can be formed by employing optimal filtering functions. These functions minimize the signal-to-distortion power ratio at a fully saturated power amplifier's output and also satisfy the Nyquist criterion. Such filtering minimizes the SNR degradation in simulated demodulation performance and distortion to the power spectral density of the transmitted signal. It is shown that the method can achieve near optimal bit error performance when a simple linear receiver is employed. Significant terminal cost reduction can be achieved in broadband wireless and satellite communications systems employing fully saturated RF power amplifiers while excellent system performance can be maintained.

Quasi-constant envelope OQPSK is presented as a design example. The square root raised cosine function with a roll-off factor $\beta \geq 0.7$ is used as the shaping pulse impulse response of a filter to form the modulated signal. For $\beta = 1$, the calculated signal-to-distortion power ratio γ obtained at the fully saturated power amplifier output is 21.38 dB. At the first null of -43 dB, the mainlobe of the power spectral density for the quasi-constant envelope OQPSK is only 77% of the bandwidth of the mainlobe of the MSK power spectral density. This performance is much better than that in broadband satellite communication systems employing linear power amplifiers [9].

The receiver is a linear receiver employing I and Q linear filters matched to the pulse shaping filters in the transmitter. Hard decision detection is employed directly at the matched filter output. At a BER of 10^{-5}, the SNR degradation is 0.1 dB when

the duration of the filter is 8 symbols and $\beta = 1$. This simulated performance is 2.3 dB better than that in [9]. Reducing the filter duration to 4 symbols causes negligible SNR degradation when $0.7 \leq \beta \leq 1$.

Rate 1/2 convolutional codes with $K = 6$ or 7 are evaluated for systems employing the quasi-constant envelope OQPSK through a fully saturated power amplifier and AWGN channel. The receiver employs filters matched only to the pulse shaping filter impulse response in the transmitter. The Viterbi decoding algorithm is used and it is shown that at a BER of 10^{-5}, the nonlinearity from the fully saturated power amplifier causes the SNR to be degraded by 0.25 dB.

Since the quasi-constant envelope OQPSK was proposed in [3], it has been implemented in several broadband satellite communication systems and significantly reduced the radio cost.

In [28], the Feher QPSK was reviewed under the same name of quasi-constant envelope modulations. To our knowledge, the phrase "quasi-constant envelope" was introduced in public for the first time in [8]. Leung and Feher [29] pointed out that the F-QPSK is a constant envelope modulation method. F-QPSK [29] suffers 1.1 dB degradation at BER = 10^{-4} and $WT_b = 0.55$, which is 1 dB inferior to the quasi-constant envelope OQPSK in this paper.

The quasi-constant envelope PSK can help to achieve near optimal demodulation performance, excellent bandwidth efficiency and significant cost reduction in broadband wireless and satellite communications systems.

REFERENCES

[1] Wildauer, E. M., Pender, M. J., Jr., and Ohlson, J. E.
Modulation method and system using constant envelope ODSCDMA with low out-of-band emissions for non-linear amplification.
U.S. Patent 5,903,555, May 11, 1999.

[2] Herbst, C. A., Fruit, L. J., Wilkerson, J. A., Jr.
Constant envelope continuous phase frequency shift key modulation apparatus and method at radio frequency.
U.S. Patent 5,812,604, Sept. 22, 1998.

[3] Liu, Q.
Performance evaluation of OQPSK and $\pi/4$ QPSK and MSK passing through a slicer.
Hughes Network Systems Technical Report, Dec. 14, 1996.

[4] Krauss, H. L., Bostian, C. W., and Raab, F. H.
Solid State Radio Engineering.
New York: Wiley, 1980.

[5] Raab, F. H., Asbeck, P., Cripps, S., Kenington, P. B., Popovic, Z. B., Pothecary, N., Sevic, J. F., and Sokal, N. O.
Power amplifiers and transmitters for RF and microwave.
IEEE Transactions on Microwave Theory and Techniques, **50** (Mar. 2002), 814–826.

[6] Weiss, M. D., Raab, F. H., and Popovic, Z.
Linearity of X-band class-F power amplifiers in high-efficiency transmitters.
IEEE Transactions on Microwave Theory and Techniques, **49** (June 2001), 1174–1179.

[7] Jacobs, I.
The effects of video clipping on the performance of an active satellite PSK communication system.
IEEE Transactions on Communication, **13** (June 1965), 195–201.

[8] Liu, Q., and Li, J.
Quasi-constant envelope OQPSK through nonlinear radio and AWGN channel.
In *Proceedings of MILCOM 2002*, vol. 1, Anaheim, CA, Oct. 7–10, 2002, 715–720.

[9] Vaughn, S., and Sorace, R.
Demonstration of the TDRS Ka-band transponder.
In *Proceedings of 2000 IEEE Military Communication Conference*, vol. 2, Los Angeles, CA, Oct. 22–25, 2000, 1055–1065.

[10] Liang, C-P., Jong, J-H., Stark, W. E., and East, J. R.
Nonlinear amplifier effects in communications systems.
IEEE Transactions on Microwave Theory and Techniques, **47** (Aug. 1999), 1461–1466.

[11] Anderson, J. B., and Sundberg, C-E. W.
Advances in constant envelope coded modulation.
IEEE Communications Magazine, **29** (Dec. 1991), 36–45.

[12] Doelz, M. I., and Heald, E. H.
Minimum shift data communication system.
U.S. Patent 2,977,417, Mar. 1961.

[13] Murota, K., and Hirade, K.
GMSK modulation for digital mobile radio telephony.
IEEE Transactions on Communications, **29** (July 1981), 1044–1050.

[14] Kaleh, G. K.
Simple coherent receivers for partial response continuous phase modulation.
IEEE Journal on Selected Areas of Communication, **7** (Dec. 1989), 1427–1436.

[15] Biglieri, E., Barberis, S., and Catena, M.
Analysis and compensation of nonlinearities in digital transmission systems.
IEEE Journal of Selected Areas of Communication, **6** (Jan. 1988), 42–51.

[16] D'Andrea, A. N., Lottici, V., and Reggiannini, R.
RF power amplifier linearization through amplitude and phase predistortion.
IEEE Transactions on Communications, **44** (Nov. 1996), 1477–1484.

[17] Farserotu, J., and Prasad, R.
A survey of future broadband multimedia satellite systems, issues and trends.
IEEE Communications Magazine, (June 2000), 128–133.

[18] Guo, N. and Milstein, L. B.
Uplink performance evaluation of multicode DS/CDMA systems in the presence of nonlinear distortions.
IEEE Journal on Selected Areas of Communication, **18** (Aug. 2000), 1418–1428.

[19] Kim, D., and Stuber, G. L.
Clipping noise mitigation for OFDM by decision-aided reconstruction.
IEEE Communications Letters, **3** (Jan. 1999), 4–6.

[20] Biglieri, E., Elia, M., and Lopresti, L.
The optimal linear receiving filter for digital transmission over nonlinear channels.
IEEE Transactions on Information Theory, **35** (May 1989), 620–625.

[21] Gusmao, A., Goncalves, V., and Esteves, N.
A novel approach to modeling of OQPSK-type digital transmission over nonlinear radio channels.
IEEE Journal on Selected Areas of Communication, **15** (May 1997), 647–655.

[22] Gersho, A., and Gray, R. M.
Vector Quantization and Signal Compression.
Boston: Kluwer, 1992.

[23] Proakis, J. G.
Digital Communications.
New York: McGraw-Hill, 2001.

[24] Liu, Q., and Li, J.
Quasi-constant envelope phase shift keying.
In *Proceedings of the 2003 Canadian Workshop on Information Theory*, Waterloo, Ontario, May 18–21, 2003, 135–138.

[25] Alberty, T.
Frequency domain interpretation of the Cramer-Rao bound for carrier and clock synchronization.
IEEE Transactions on Communications, **43** (Feb./Mar./Apr. 1995), 1185–1191.

[26] Viterbi, A. J.
Principles of Coherent Communication.
New York: McGraw-Hill, 1966.

[27] Heller, J. A., and Jacobs, I. M.
Viterbi decoding for satellite and space communication.
IEEE Transactions on Communications, **19** (Oct. 1971), 835–848.

[28] Simon, M.
Bandwidth Efficient Digital Modulation with Application to Deep Space Communications.
New York: Wiley, 2003.

[29] Leung, P. S. K., and Feher, K.
F-QPSK—A superior modulation technique for mobile and personal communications.
IEEE Transactions on Broadcasting, **39** (June 1993), 288–294.

Jia Li (M'02) received the B.S. degree in electronics and information systems from Peking University, Beijing, China, in 1996, the M.S.E. degree and the Ph.D. degree both in electrical engineering from the University of Michigan, Ann Arbor, in 1997 and 2002.

Dr. Li is an Assistant Professor of Engineering with Oakland University, Rochester, MI. Her research interests include communication theory, statistical shape modeling, image segmentation, multimodal image registration, image-guided therapy.

Qingchong Liu (S'93—M'99) received the B.S. degree in electronics and information systems from Peking University, Peking, China, in 1990, the M.S. degree in electrical engineering from New Mexico State University, Las Cruces, in 1993, and the Ph.D. degree in electrical engineering from the University of Southern California, Los Angeles, in 1996.

He was a senior member of the technical staff with Hughes Network Systems from 1996 to 2000. He joined Oakland University, Rochester, MI, in 2000, where he is an Associate Professor of Engineering. His research interests include radio network security, communications networks, ultrawideband communications, optical wireless communications, modulation and coding, synchronization, signal design and detection.

Dr. Liu has a patent in frequency synchronization for global mobile satellite networks using low/medium Earth orbit satellites, and designed modulation, signal detection, and multiple access protocols for 3 launched international programs.